Transport Mechanisms in Metallic and Semiconducting Single-Wall Carbon Nanotube Networks

Kazuhiro Yanagi,[†,*] Hiroki Udoguchi,[†] Satoshi Sagitani,[†] Yugo Oshima,[‡] Taishi Takenobu,[§] Hiromichi Kataura,[⊥,∥] Takao Ishida,[¶] Kazuyuki Matsuda,[†] and Yutaka Maniwa[†,∥]

[†]Department of Physics, Tokyo Metropolitan University, Hachioji, 192-0397 Tokyo, Japan, [‡]RIKEN, Wako, 351-0198 Saitama, Japan, [§]Department of Applied Physics, Waseda University, Shinjyuku, 169-8050 Tokyo, Japan, [⊥]Nanotechnology Institute, Advanced Industrial Science and Technology (AIST), Tsukuba, 305-8562 Ibaraki, Japan, [∥]CREST, Japan Science Technology Agency, Saitama 332-0012, Japan, and [¶]Ubiquitous MEMS and Micro Engineering Research Center, AIST, Tsukuba, 305-8562 Ibaraki, Japan

ABSTRACT A fundamental understanding of the conduction mechanisms in single-wall carbon nanotube (SWCNT) networks is crucial for their use in thin-film transistors and conducting films. However, the uncontrollable mixture state of metallic and semiconducting SWCNTs has always been an obstacle in this regard. In the present study, we revealed that the conduction mechanisms in nanotube networks formed by high-purity metallic and semiconducting SWCNTs are completely different. Quantum transport was observed in macroscopic networks of pure metallic SWCNTs. However, for semiconducting SWCNT networks, Coulomb-gap-type conduction was observed, due to Coulomb interactions between localized electrons. Crossovers among a weakly localized state and strongly localized states with and without Coulomb interactions were observed for transport electrons by varying the relative content of metallic and semiconducting SWCNTs. It was found that hopping barriers, which always exist in normal SWCNT networks and are serious obstacles to achieving high conductivity, were not present in pure metallic SWCNT networks.

KEYWORDS: carbon nanotube · transport mechanisms · metallic and semiconducting types · variable range hopping · weak localization

Single-wall carbon nanotubes (SWCNTs) are cylindrical graphitic tubes with diameters of about 1 nm. They exhibit metallic or semiconducting characteristics depending on how the graphitic sheets are rolled (chirality). Because of their remarkable electric characteristics, SWCNTs are expected to be used in a wide range of applications such as field-effect transistors and conducting films.[1] In such applications, carrier transport occurs in networks of SWCNTs. Thus, a fundamental understanding of the electric transport properties in such networks is critical. A number of studies concerning this issue have been reported.[2−6] In a single bundle of nanotubes, it has been suggested that conductance is affected by two-dimensional weak localization processes,[7] due to the interference of electron waves, which are classified as quantum transport phenomena. However, the observed temperature dependence of resistance in nanotube networks, which are networks formed by nanotube bundles, has been mainly explained by variable range hopping (VRH) models that assume strong localization of electrons, indicating the presence of strong disorder at contact points between the bundles.[2−4,6] These previous studies were performed on networks with an uncontrolled mixture of metallic and semiconducting SWCNTs. Apparently, the presence of semiconducting SWCNTs impedes good conduction and introduces a high degree of disorder. It has been reported that chemical doping of nanotube networks can change the conduction mechanisms;[8] however, for the reported pure SWCNT networks, phonon-assisted hopping processes were found to play a major role in conduction. In the case of metallic nanowires and nanograins, although boundaries exist between the wires and grains, quantum transport has been observed in macroscopic networks of such structures.[9] However, it has not yet been established whether such transport is possible in the absence of intentional chemical treatment on nanotube networks. Recently, effective metallic−semiconducting separation has been achieved, allowing the formation of high-purity networks.[10] Thus, in this study, we investigated how the presence of semiconducting types affects the conduction mechanisms in SWCNT networks. We observed that the transport mechanisms systematically changed as the relative content of metallic to semiconducting SWCNTs (MS ratio) was varied. We found that quantum transport was achieved in macroscopic networks of pure metallic SWCNTs.

*Address correspondence to yanagi@phys.metro-u.ac.jp.

Received for review May 27, 2010 and accepted June 24, 2010.

Published online July 1, 2010.
10.1021/nn101177n

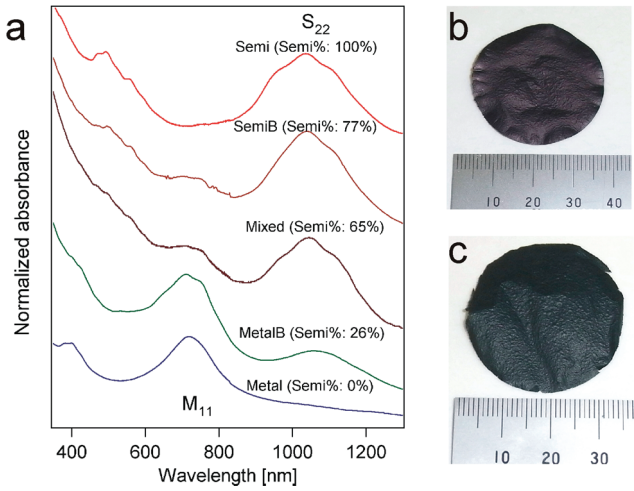

Figure 1. (a) Optical absorption spectra of five SWCNT samples, Metal, MetalB, Mixed, SemiB, and Semi, with different MS ratios. The MS ratio (Semi%) was determined as described in the text. Photos of sheets of high-purity (b) metallic and (c) semiconducting SWCNT buckypaper.

We prepared five sheets of SWCNT buckypaper with controlled MS ratios (Figure 1). Optical absorption spectra of the five samples, which were dispersed in 1% deoxycholate sodium salt solutions from the sheets, are shown in Figure 1a. Figure 1b,c shows example images of the sheets of high-purity metallic (referred to as Metal) and semiconducting (referred to as Semi) SWCNT buckypaper, respectively. These samples were produced by a careful purification process followed by metal−semiconductor separation using density gradient ultracentrifugation of SWCNTs initially produced by an arc-discharge method (Meijo-Nanocarbon Co.).[11,12] The average diameter of the nanotubes was estimated to be about 1.46 nm from X-ray diffraction profiles (Supporting Information Figure S.1). The average diameter of the nanotube's bundles in the sheets was estimated to be approximately 10 nm (Supporting Information Figure S.1). In the SWCNT buckypaper sheets, the amount of residual metals and other contaminants was determined to be less than 1% by weight from X-ray photoelectron spectroscopy (XPS) (Supporting Information Figure S.2), and the residual magnetic metal impurity content was negligible at ~30 ppma (Supporting Information Figure S.3). The residual amount of surfactants, such as deoxycholate sodium salt, was less than the detection limit of XPS and FT-IR measurements because the presence of sodium was not detected in the XPS spectra (Figure S.2 of Supporting Information) and no specific peaks from surfactants were observed in FT-IR measurements (Figure S.4 of Supporting Information). The densities of the sheets were found to be consistent at $(4.82 \pm 0.78) \times 10^5$ g m^{-3}. *G*/*D* ratio in a Raman spectrum of a SWCNT sample was estimated to be 20 (Supporting Information Figure S.5).

As seen in the optical absorption spectra of the high-purity samples (Metal and Semi) shown in Figure 1a, no bands associated with the other conduction type could be identified, indicating a purity of more than 95%. The relative contents of semiconducting SWCNTs (Semi%) in the Metal and the Semi samples were defined here as 0 and 100%, respectively. The MS ratio of the remaining three samples was evaluated from the ratio of the intensity of the M_{11} and S_{22} optical absorption bands (here S_{ii} and M_{ii} indicates the *i*th optical transition of the metallic and semiconducting SWCNTs) as follows. The Semi% of these intermediate samples was estimated by a linear combination of the optical absorption spectra of the Metal and the Semi. Therefore, although there are several approaches to evaluate the relative intensities of the metallic and the semiconducting SWCNTs,[13] we did not perform any artificial subtraction of π-plasmon effect for the evaluation of Semi%. Consequently, the Semi% values for the five sheets were determined to be 0% (Metal), 26% (MetalB), 65% (Mixed), 77% (SemiB), and 100% (Semi), within an error of a few percent. Here we use a term "Semi% = 100%" for the Semi sample; this does not directly mean that the content of metallic SWCNTs in Semi was zero. The relationship between Semi% and the relative volume of semiconducting SWCNTs (or the amount of residual metallic SWCNTs) is discussed later in reference to temperature dependence of resistance. Resistance and magneto-resistance (MR) measurements were performed on approximately 10 mm × 5 mm × 10 μm (thickness) samples of the sheets using a physical properties measurement system (PPMS, Quantum Design Co.) with a four-probe method using Au wires (diameter = 0.1 mm) at pressure contact. The distance between the wires was approximately 2 mm. Prior to the measurements, the samples were annealed at 500 °C for 1 h at 10^{-6} Torr. Measurements were performed under a He atmosphere.

Figure 2a shows the resistivity of the Metal and Semi samples as a function of temperature. In the Metal sample, the resistivity was almost constant as the temperature decreased; however, in the Semi sample, the resistance rapidly increased and became more than 10 MΩ (beyond our instrumentation limit) at 4 K, indicating the insulating properties of the Semi network at low temperature. The resistivity of the Semi network was almost 7 orders of magnitude larger than that of the Metal network at low temperature, clearly indicating that a different transport mechanism is involved. In our samples, d*R*/d*T* is always negative between $T = 3$ and 380 K, suggesting a high degree of intertubular coupling.[2] The resistivity of the five samples with different MS ratios are summarized in Supporting Information Figure S.6.

Figure 2b shows the temperature dependence of resistance normalized by the resistance value at $T = 380$ K for the five samples with different MS ratios. It can be seen that all of the curves appear different from each other. At low temperature, the normalized resistance becomes lower as the content of semiconducting

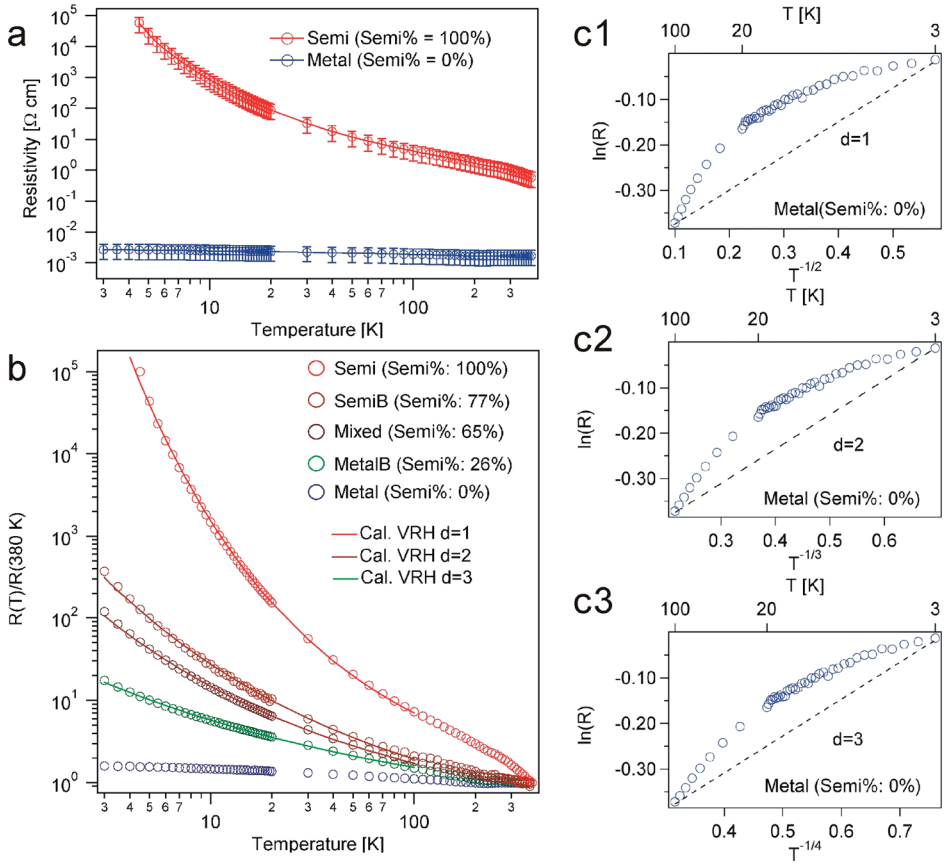

Figure 2. (a) Resistivity in sheets of high-purity metallic (Metal, Semi% = 0%) and semiconducting (Semi, Semi% = 100%) SWCNT buckypaper as a function of temperature. (b) Normalized resistance of five different samples with different MS ratios as a function of temperature, Semi (red circles), SemiB (brown circles), Mixed (dark-brown circles), MetalB (green circles), and Metal(blue circles). The data for the Semi sample could be reproduced using the VRH model with $d = 1$ (red line), that for the SemiB and Mixed samples using VRH with $d = 2$ (brown lines), and that for MetalB by VRH with $d = 3$ (green line). Further details are shown in Supporting Information Figure S.7. (c1−c3) Natural logarithm of resistance of the Metal sample plotted as a function of $T^{-1/2}$, $T^{-1/3}$, and $T^{-1/4}$, respectively. If the resistance could be reproduced by VRH models with any d value, the natural logarithm of resistance should show a linear dependence on $T^{-1/2}$, $T^{-1/3}$, or $T^{-1/4}$ (dotted lines for guide). However, the resistance of the Metal sample did not show such behavior, indicating that the conduction could not be explained by VRH.

SWCNTs decreases. Contact points between nanotubes or between nanotube bundles would be expected to disrupt smooth conduction by acting as scattering centers and potential barriers. Although the number of such disorders depends on the densities and lengths of the nanotubes and nanotube bundles, the effects of these variations can be eliminated by evaluating the normalized resistance. Thus, the observed differences in the normalized resistance indicate that changing the MS ratio affects the intrinsic physical properties of the disorders.

Next, we analyzed the temperature dependence of the resistance using VRH models based on the following equation:[14]

$$R(T) = R_0 \exp\left[\left(\frac{T_0}{T}\right)^{1/(d+1)}\right]$$

Here, d has a value of either 2 or 3 in Mott-VRH, reflecting the dimensionality of a system in which electrons hop (VRH model proposed by Mott, which is referred to simply as VRH),[14] or 1 in ES-VRH, reflecting the existence of a Coulomb gap due to Coulomb interactions between localized electrons (Coulomb gap VRH by Efros and Shklovskii).[15] T_0 is a characteristic temperature used in the VRH model. The analysis results are shown in Figure 2b, and the details are depicted in Supporting Information Figure S.7. In the Semi sample, the temperature dependence could be reproduced by the model with $d = 1$, which indicates the presence of Coulomb interactions between localized electrons, inducing a Coulomb gap in the density of states of conduction (ES-VRH).[15] However, in the SemiB and Mixed samples, the appropriate value of d was 2, and in the MetalB sample, it was 3. Remarkably, for the Metal sample, the dependence could not be fitted with any value of d in the range of 1−3 (Figure 2c). The physical mechanism of conduction in the Metal sample will be discussed later in reference to the MR results. The relationship between the d values and Semi% is summarized in Figure 4.

We first consider conduction in pure semiconducting SWCNT networks, which was found to occur by the ES-VRH mechanism ($d = 1$). This type of conduction has

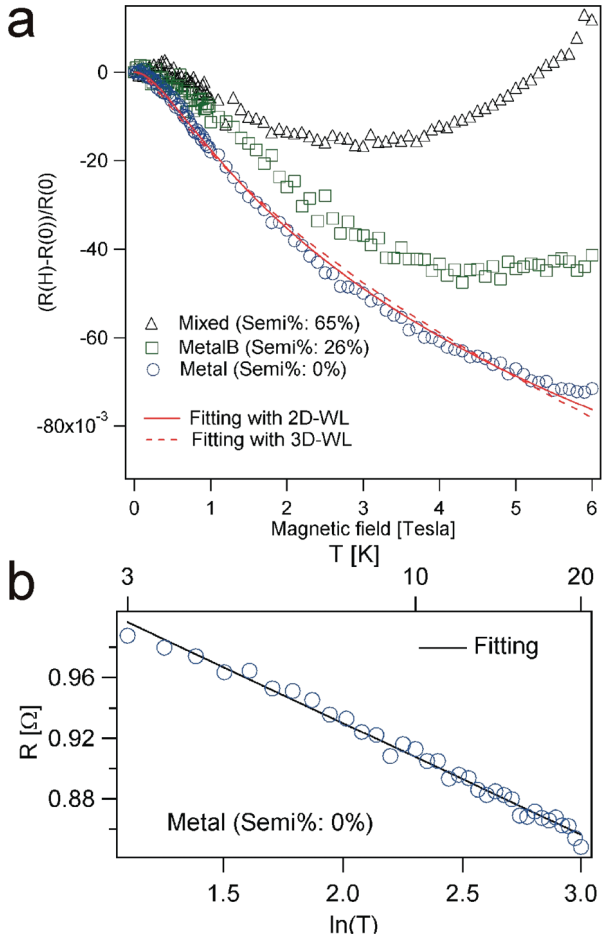

Figure 3. (a) Magneto-resistance in nanotube networks for three samples with different MS ratios. Blue circles, green squares, and black triangles indicate data for Metal (Semi% = 0%), MetalB (Semi% = 26%), and Mixed (Semi% = 65%) samples, respectively. Solid and dotted red lines indicate the fitting results using 2D weak localization (WL) and 3D WL models, respectively. (b) Resistance of Metal sample exhibits logarithmic dependence on temperature. Experimental data (blue circles) and a linear fitting result for the guide (solid line).

already been reported in networks with a small volume fraction (less than 8%) of SWCNTs embedded among insulating polymers[6,16] or in high-resistivity nanotube networks produced by annealing at a relatively high temperature.[8] As the resistance of the Semi sample indicates, semiconducting SWCNTs can be regarded as insulating materials at low temperature. Therefore, on the basis of theoretical studies on the transition between ES-VRH and VRH,[16,17] the conduction process in the Semi sample can be explained in the following manner. In semiconducting SWCNTs, uncontrolled donors and acceptors lead to random charging of the metallic SWCNTs within the bundles. When the content of metallic SWCNTs is small, Coulomb interactions between electrons of distant metallic SWCNTs induce a soft Coulomb gap in the density of states of conduction. Therefore, the ES-VRH conduction occurs. However, when the content of metallic SWCNTs increases, these SWCNTs enhance the screening of the Coulomb potential,[16] which results in a weakening of Coulomb interactions, and the conduction mechanism changes from ES-VRH to the conventional VRH. This theoretical prediction is in good agreement with our observation that an increase in the content of metallic SWCNTs changed the conduction mechanism from ES-VRH ($d = 1$) to VRH ($d = 2$ or 3).

Therefore, conduction in the Semi sample is assumed to be caused by hopping between residual metallic SWCNTs that could not be detected in the optical absorption spectra. Benoit *et al.* proposed that the volume fraction of SWCNTs, which were in a mixed metallic and semiconducting state, can be estimated from the T_{ES} value (defined as the value of T_0 for $d = 1$).[6] Theoretically, for a concentration n of metallic wires of length L, $T_{ES} \propto 1/(nL^3)^2$.[16] The T_{ES} value of the Semi sample in this study was determined to be 650 K. From the data reported by Benoit *et al.* (the ratio of metallic to semiconducting SWCNTs in their samples is assumed to be 1 to 2), this T_{ES} value indicates that the volume fraction of metallic SWCNTs is less than about 1%, supporting the high purity of the Semi sample.

As the content of metallic SWCNTs increases, the value of d becomes large. Such a systematic change in the d value is also observed in mixed systems of conducting and insulating polymers.[18,19] For example, the relative content of conducting polymers mixed in insulating polymers influences the value of d, and the d values varies from 1 to 3 as the content of the conducting polymer is increased.[18,19] The physical reasons for this is still a matter of some discussion,[18,19] but we suggest that the enhancement of conduction channels caused by the increase in metallic SWCNT content is one origin for the systematic change in d.[20] As mentioned before, the amount of residual surfactants was less than the detection limit of XPS and FT-IR measurements (Supporting Information); however, unidentified residual surfactants might influence the transport properties of SWCNTs, but in this study, while we applied the same washing procedures on all of the samples, we systematically changed the MS ratio in the samples. Thus, the observed changes on the transport mechanisms were assumed to be caused by the changes of the MS ratio, not by such unidentified residual surfactants. As mentioned above, there are some similarities between the conduction mechanisms in conducting polymers and SWCNTs. However, while the transport mechanisms in conducting polymers can be explained by VRH conduction for any volume fraction,[18,19] conduction in the pure metallic SWCNT network cannot be explained by a simple VRH scenario (Figure 2c). To clarify the conduction mechanism in the latter case, we carried out MR measurements on the samples.

Figure 3a shows MR data for the Metal (Semi% = 0%), MetalB (Semi% = 26%), and Mixed (Semi% = 65%) samples. The MR of the Mixed sample is negative for low magnetic fields, followed by the positive upturn in a high magnetic field region. Such phenomena are

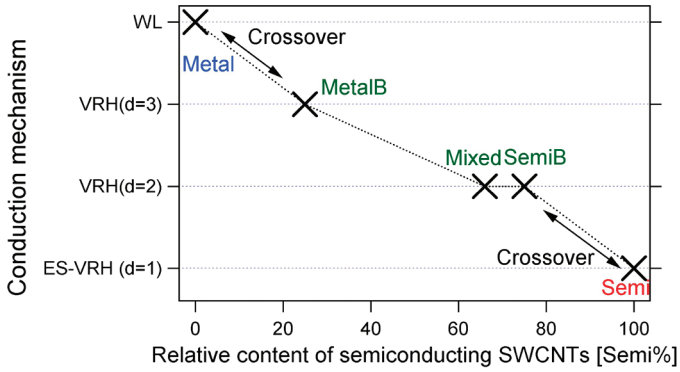

Figure 4. Phase diagram of conduction mechanisms in SWCNT networks as a function of MS ratio. Relationship among relative content of semiconducting SWCNTs (Semi%), *d* values in VRH analyses, and conduction mechanisms. Weak localization: WL. Variable range hopping: VRH. Coulomb gap VRH by Efros & Shklovskii: ES-VRH.

consistent with previous studies.[2] Kim *et al.* studied magneto-transport phenomena using several theoretical models[2] and concluded that the positive and negative MR are caused by VRH and weak localization, respectively. Remarkably, the positive upturn in the MR decreases with decreasing Semi%, and no such upturn occurs for the Metal sample. This suggests that weak localization is the dominant factor for conduction in the Metal sample. These MR results clearly indicate that hopping processes were reduced in the Metal sample, which agrees with the temperature dependence of the resistance.

The MR of the Metal sample is well reproduced by two-dimensional weak localization theory using the following equation:[21]

$$\Delta\sigma(H) = \frac{e^2}{2\pi^2\hbar^2}\left[\ln x + \varphi\left(\frac{1}{2} + \frac{1}{x}\right)\right]$$

Here $x = 4L_{th}^2eH/\hbar c$, and L_{th} is the decoherence length (effective scale size for quantum interference effects).[9] L_{th} was determined to be 26 nm from the fitting. We also tried to fit the data using a three-dimensional weak localization model.[22] As shown in Figure 3a, the two-dimensional model produces a somewhat better fit than the three-dimensional model. The resistance of the Metal sample exhibits a logarithmic dependence on T at low temperature, as shown in Figure 3b, supporting the two dimensionality of the weak localization processes. The bundle sizes of metallic nanotubes were determined to be approximately 10 nm (Supporting Information Figure S.1). This is less than the estimated decoherence length; therefore, it would lead to two-dimensional rather than three-dimensional electron conduction. Thus, we assume that the anisotropy of the nanotube bundles influenced the dimensionality of the weak localization.

In summary, the conduction mechanisms in SWCNT networks are depicted as a function of MS ratio in Figure 4. The figure is a phase diagram indicating crossovers between the conduction mechanisms, from quantum transport, VRH, and ES-VRH, as a function of MS ratio. Increasing Semi% first causes a transition from weak localization (WL) to VRH and then from VRH to ES-VRH. As mentioned by Anderson,[23] a crossover from the weak to strong localization regimes occurs as the strength of disorders increases. In SWCNT networks, we revealed that the characteristics of the disorders can be controlled by varying the MS ratio. The presence of semiconducting SWCNTs was found to be the main factor causing localization of the conduction electrons. One of the possible origins for strong disorders is the Schottky barriers between metallic and semiconducting SWCNTs. Another possibility is the potential barriers among semiconducting SWCNTs due to the random distribution of nanotube diameters and the resulting inconsistence of band gap energies. In pure metallic SWCNT networks, boundaries between the nanotubes or bundles act as weak sources of disorder, and as a result, quantum transport was achieved in such macroscopic networks. The revealed phase diagram will become the basis of a general concept for understanding the conduction mechanisms in macroscopic networks of not only SWCNTs but also nanoparticles with various electronic structures.

METHODS

Preparation of Sheets of SWCNT Buckypaper with Different MS Ratios and Evaluation of Their Characteristics. We used density gradient ultracentrifugation (DGU), which was first suggested by Arnold *et al.*,[11] to obtain SWCNTs with different MS ratios. We revised their method and used deoxycholate sodium salt (DOC) as an additional co-surfactant.[12,24] SWCNTs (Arc-SO, Meijo-Nanocarbon Co.) were dispersed into 1 or 2% DOC solutions, and SWCNTs with different MS ratios were obtained through DGU processes in experimental setups similar to that described in our previous papers.[12,24] Obtained SWCNT solutions were carefully washed several times with methanol, hot water, and toluene, and then the sheets of buckypaper were prepared. The details of the preparation and the washing procedures are described in Supporting Information. Optical absorption spectra were measured using a UV−vis spectrophotometer (Shimazu UV-3600). Thickness of the sheets was evaluated by a digital micrometer (Mitutoyo Co., MDC-25MJ).

Acknowledgment. This work was partially supported by a Grant-in-Aid for Scientific Research on Innovative Areas (No. 21108523, "pi-Space") from the Ministry of Education, Culture, Sports, Science and Technology, and by Industrial Technology Research Grant Program in 2007 from New Energy and Industrial Technology Development Organization, Japan.

Supporting Information Available: X-ray diffraction profiles of high-purity metallic SWCNTs, XPS spectra of purified SWCNTs used in this study, magnetic characteristics of high-purity metal-

lic SWCNTs, FT-IR and Raman spectra of purified SWCNTs, resistivity of the sheets of all SWCNT samples used this study, details of analysis results by VRH on Semi, SemiB, Mixed, and MetalB samples, details of procedures to prepare high-purity metallic and semiconducting SWCNTs, and details of washing procedures of SWCNTs after density gradient separations. This material is available free of charge *via* the Internet at http://pubs.acs.org.

REFERENCES AND NOTES

1. Baughman, H.; Zakhidov, A. A.; de Heer, W. A. Carbon Nanotubes—The Route toward Applications. *Science* **2002**, *297*, 787–792.
2. Kim, G. T.; Choi, E. S.; Kim, D. C.; Suh, D. S.; Park, Y. W.; Liu, K.; Duesberg, G.; Roth, S. Magnetoresistance of an Entangled Single-Wall Carbon Nanotube Network. *Phys. Rev. B* **1998**, *58*, 16064–16069.
3. Yosida, Y.; Oguro, I. Variable Range Hopping Conduction in Bulk Samples Composed of Single-Walled Carbon Nanotubes. *J. Appl. Phys.* **1999**, *86*, 999–1003.
4. Takano, T.; Takenobu, T.; Iwasa, Y. Enhancement of Carrier Hopping by Doping in Single Walled Carbon Nanotube Films. *J. Phys. Soc. Jpn.* **2008**, *77*, 124709–124713.
5. Skakalova, V.; Kaiser, A. B.; Osvath, Z.; Vertesy, G.; Biro, L. P.; Roth, S. Ion Irradiation Effects on Conduction in Single-Wall Carbon Nanotube Networks. *Appl. Phys. A: Mater. Sci. Process.* **2008**, *90*, 597–602.
6. Benoit, J. M.; Corraze, B.; Chauvet, O. Localization, Coulomb Interactions, and Electrical Heating in Single-Wall Carbon Nanotubes/Polymer Composites. *Phys. Rev. B* **2002**, *65*, 241405–241408.
7. McIntosh, G. C.; Kim, G. T.; Park, J. G.; Krstic, V.; Burghard, M.; Jhang, S. H.; Lee, S. W.; Roth, S.; Park, Y. W. Orientation Dependence of Magneto-Resistance Behaviour in a Carbon Nanotube Rope. *Thin Solid Films* **2002**, *417*, 67–71.
8. Vavro, J.; Kikkawa, J. M.; Fischer, J. E. Metal-Insulator Transition in Doped Single-Wall Carbon Nanotubes. *Phys. Rev. B* **2005**, *71*, 155410–155420.
9. Lee, P.; Ramakrishnan, T. Disordered Electronic Systems. *Rev. Mod. Phys.* **1985**, *57*, 287–337.
10. Hersam, M. Progress towards Monodisperse Single-Walled Carbon Nanotubes. *Nat. Nanotechnol.* **2008**, *3*, 387–394.
11. Arnold, M.; Green, A.; Hulvat, J.; Stupp, S.; Hersam, M. Sorting Carbon Nanotubes by Electronic Structure Using Density Differentiation. *Nat. Nanotechnol.* **2006**, *1*, 60–65.
12. Yanagi, K.; Miyata, Y.; Kataura, H. Optical and Conductive Characteristics of Metallic Single-Wall Carbon Nanotubes with Three Basic Colors; Cyan, Magenta, and Yellow. *Appl. Phys. Express* **2008**, *1*, 034003–034005.
13. Landi, B. J.; Ruf, H. J.; Evans, C. M.; Cress, C. D.; Raffaelle, R. P. Purity Assessment of Single-Wall Carbon Nanotubes, Using Optical Absorption Spectroscopy. *J. Phys. Chem. B* **2005**, *109*, 9952–9965.
14. Mott, N. *Conduction in Non-Crystalline Materials*; Oxford University Press: Oxford, 1987; pp 27−29.
15. Shklovskii, B. I.; Efros, A. *Electronic Properties of Doped Semiconductors*; Springer-Verlag: Berlin, 1984; pp 228−244.
16. Hu, T.; Shklovskii, B. Theory of Hopping Conductivity of a Suspension of Nanowires in an Insulator. *Phys. Rev. B* **2006**, *74*, 054205–054209.
17. Zhang, J.; Shklovskii, B. Density of States and Conductivity of a Granular Metal or an Array of Quantum Dots. *Phys. Rev. B* **2004**, *70*, 115317–115329.
18. Reghu, M.; Yoon, C.; Yang, Y.; Moses, D.; Smith, P.; Heeger, A.; Cao, Y. Transport in Polyaniline Networks near the Percolation Threshold. *Phys. Rev. B* **1994**, *50*, 13931–13941.
19. Planès, J.; Wolter, A.; Cheguettine, Y.; Proň, A.; Genoud, F.; Nechtschenin, M. Transport Properties of Polyaniline-Cellulose-Acetate Blends. *Phys. Rev. B* **1998**, *58*, 7774–7785.
20. Shante, V. Hopping Conductin in Quasi-One-Dimensional Disordered Compounds. *Phys. Rev. B* **1977**, *16*, 2597–2612.
21. Hikami, S.; Larkin, A.; Nagaoka, Y. Spin−Orbit Interaction and Magnetoresistance in the Two Dimensional Random System. *Prog. Theor. Phys.* **1980**, *63*, 707–710.
22. Kawabata, A. Theory of Negative Magnetoresistance in Three-Dimensional Systems. *Solid State Commun.* **1980**, *34*, 431–432.
23. Anderson, P. W.; Abrahams, E.; Ramakrishnan, T. V. Possible Explanation of Nonlinear Conductivity in Thin-Film Metal Wires. *Phys. Rev. Lett.* **1979**, *43*, 718–720.
24. Yanagi, K.; Yasumitsu, M.; Liu, Z.; Suenaga, K.; Okada, S.; Kataura, H. Influence of Aromatic Environments on the Physical Properties of β-Carotene. *J. Phys. Chem. C* **2010**, *114*, 2524–2530.